Pulse Asymptotics of Three-Dimensional Baroclinic Waves

BRIAN F. FARRELL

Center for Earth and Planetary Physics, Harvard University, Cambridge, MA 02138

(Manuscript received 5 October 1982, in final form 24 May 1983)

ABSTRACT

The asymptotic development at large time of waves arising from localized disturbances in a baroclinic flow is examined.

Vertical structures unlike those associated with the more commonly examined temporal normal modes are found both for the pulse confined to a channel as previously examined and for the unconfined pulse on an infinite β-plane. These structures and their implied transports are compared to observations in the regions of storm tracks.

It is also found that the meridional extent of the asymptotic solution becomes large compared to observed cyclone wavetrains, emphasizing the importance of flow inhomogeneity and sphericity effects in determining the latitudinal structure of eddies.

1. Introduction

The process by which the potential energy of the vertically sheared atmospheric zonal flow is transferred to the scale of synoptic weather systems was first described in the work of Charney (1947) and Eady (1949). The method of analysis used by these authors is that of normal modes: the quasi-geostrophic equations are linearized about a zonal flow with vertical shear; periodic solutions are assumed in the zonal and meridional; and a vertical structure equation is obtained for the mode on which the boundary conditions induce an eigenvalue relation for the complex phase speed. The structure of the unstable modes is a uniform periodic array of highs and lows growing exponentially in time. This analysis need not, however, be restricted to real wavenumber with spatially periodic structure as the dispersion relation can be continued into the complex plane with the general solution displaying spatial as well as temporal growth corresponding to complex spatial wavenumbers in addition to complex phase speeds. Purely spatial growth has been successful in analyzing experiments with boundary layer flow forced at a point (Gaster, 1965) and has been applied to Gulf Stream instabilities (Hogg, 1976; Thacker, 1976).

The pulse solution, which is the linear asymptotic response of the unstable fluid to a localized excitation, combines both temporal and spatial growth. The simplest case is that of a fixed meridional mode, confining the spatial growth to the zonal direction. This would be appropriate for a narrow channel because the instability is maximized by the gravest mode which can be expected to rapidly dominate the meridional structure. Observation suggests that midlatitude jetstreams confine waves to a few Rossby radii and the GCM experiments of Simmons and Hoskins (1979) may be interpreted as similar to Charney mode pulses confined to a channel with the jet stream width (Farrell, 1982a; hereafter F1).

This work extends these results by determining the vertical structure of the waves that make up the pulse both in the channel and on an infinite β-plane and by examining how the meridional structure is set up in the absence of boundary influence. The vertical structure is found to be different in some cases from that expected by intuition grounded in familiarity with temporal normal modes, and to be more in accord with observations upstream and downstream of the major stormtracks.

The three-dimensional pulse solutions indicate how rapidly a point excitation can be expected to fill a channel and therefore how soon the channel solutions become valid. In addition, these solutions address the question of what determines the meridional scale of the eddies. This debate has a long history (Stone, 1969; McIntyre, 1970) with the effects of sphericity and the finiteness of the jet implicated in various combinations. It would seem that the fundamental background to this debate must be the solution arising from a point excitation on a β-plane. We find the disturbance is confined in latitude compared to its zonal propagation but not by enough to prevent the jet from exerting an important influence.

It should be noted that the solutions are of interest whether or not a pure realization of the pulse is seen in observations, as it is likely that at any point in a baroclinic wave train the local wave will exhibit a combination of growth and decay in space and time so that the vertical structure and accompanying transports

implied by these complex wavenumbers should be often found. Therefore, the analysis is not restricted in interpretation to the asymptotic pulse.

2. Method

The longtime asymptotic disturbance produced by a localized excitation may be obtained systematically by a simultaneous deformation of the inversion contours of a combined Fourier/Laplace transform in wavenumber and frequency in such a way as to identify the pinch singularity with the maximum temporal growth. This technique was developed in the plasma literature (Briggs, 1964) and used by Merkine (1977) and Merkine and Shafranek (1980) in an investigation of the asymptotics of the two level model. The method was outlined in connection with the Charney problem in F1. It is equivalent to the method of steepest descents used by Gaster and Davy (1968) with the advantage of providing a systematic identification of the saddles which contribute to the inversion. The reader is referred to these sources for the derivation of the asymptotic streamfunction:

$$\psi(x, y, z, t) \sim \psi_{k^*,l^*,\omega^*}(z) \times \frac{\exp\left\{i\left[k^*\frac{x}{t} + l^*\frac{y}{t} - \omega^*\right]t\right\}}{t\left[\frac{\partial^2\omega^*}{\partial k^{*2}}\frac{\partial^2\omega^*}{\partial l^{*2}} - \left(\frac{\partial^2\omega^*}{\partial k^*\partial l^*}\right)^2\right]^{1/2}}, \tag{1}$$

where the solution has been assumed to have the form $\psi_{k,l,\omega}(z)e^{i(kx+ly-\omega t)}$. A phase factor has been neglected and the following identifications made:

$\psi_{k,l,\omega}(z)$	the vertical structure at k, l, ω of the perturbation geostrophic stream function
k	complex zonal wavenumber
l	complex meridional wavenumber
ω	complex frequency
x	eastward (zonal) distance
y	northward distance
z	height
$(x/t, y/t)$	ray along which the asymptotic is evaluated.

The wavenumbers and frequency are understood to be related by the dispersion relation:

$$\Delta(k, l, \omega) = 0, \tag{2}$$

and contributions are from points where:

$$\left.\begin{aligned}\frac{x}{t} &= \frac{\partial\omega^*}{\partial k}(k^*, l^*)\\ \frac{y}{t} &= \frac{\partial\omega^*}{\partial l}(k^*, l^*)\end{aligned}\right\}. \tag{3}$$

Following Gaster and Davey (1968), and Merkine and Shafranek (1980), the above three-dimensional expression may be reduced to an equivalent two-dimensional one by use of the transformation of Squire (1933):

$$\psi(x, y, z, t) \sim \psi_{\alpha^*,\Omega^*}(z) \frac{\alpha^* \exp\left\{i\alpha^*\left[\left(\frac{x}{t} - \frac{\Omega^*}{\alpha^*}\right)^2 + \left(\frac{y}{t}\right)^2\right]^{1/2}t\right\}}{t\left[\left(\alpha^*\frac{x}{t} - \Omega^*\right)\frac{d^2\Omega}{d\alpha^2}\Big|_{\alpha^*,\Omega^*} - \left(\frac{x}{t} - \frac{d\Omega}{d\alpha}\Big|_{\alpha^*,\Omega^*}\right)^2 - \left(\frac{y}{t}\right)^2\right]^{1/2}}, \tag{4}$$

where $\alpha^2 = k^2 + l^2$,

$$\frac{\Omega}{\alpha} = \frac{\omega}{k}, \tag{5}$$

and (3) may be shown to require

$$\left(\frac{x}{t} - \frac{\Omega^*}{\alpha^*}\right)\left(\frac{x}{t} - \frac{d\Omega^*}{d\alpha^*}\right) + \left(\frac{y}{t}\right)^2 = 0, \tag{6}$$

which identifies the points Ω^*, α^* that contribute to the asymptotic solution (4).

We shall be concerned with the leading order asymptotic given by the exponential in (4), except to note possible caustic points where the denominator in (4) vanishes. The pulse shape is symmetric about $y/t = 0$ in the x/t, y/t plane and exhibits exponential growth:

$$\gamma_i = R_e\left\{i\alpha^*\left[\left(\frac{x}{t} - \frac{\Omega^*}{\alpha^*}\right)^2 + (y/t)^2\right]^{1/2}\right\}, \tag{7}$$

level curves of γ_i in the x/t, y/t plane can be viewed as the logarithm of pulse amplitude in the x,y plane at some instant of time.

All that is required to obtain the asymptotic pulse is a dispersion relation (2) which is valid in the complex plane.

3. Formulation of the baroclinic instability problem

The behavior of small perturbations to a baroclinic fluid in zonal flow is governed by the linearized equation expressing the conservation of pseudo potential vorticity (Pedlosky, 1979):

$$\left(\frac{\partial}{\partial t} + U\frac{\partial}{\partial x}\right)q + \frac{\partial\psi}{\partial x}\frac{\partial\Pi}{\partial y} = 0. \tag{8a}$$

Sufficient boundary conditions require the vertical velocity to vanish on rigid horizontal surfaces or the streamfunction decay as $z \to \infty$ to satisfy a radiation condition if unbounded above:

$$\left(\frac{\partial}{\partial t} + U\frac{\partial}{\partial x}\right)\frac{\partial \psi}{\partial z} - \frac{\partial U}{\partial z}\frac{\partial \psi}{\partial x} = 0,$$

$$z = 0, z_T; \quad \psi(z) \to 0, \quad z \to \infty, \tag{8b}$$

where

$U(z)$ = basic state zonal velocity.
$q = \nabla^2\psi + \rho^{-1}\partial/\partial z(\epsilon\rho\partial\psi/\partial z)$, perturbation potential vorticity
$\epsilon = f^2/N^2$, square ratio of the Coriolis parameter to the Brunt–Väisälä frequency
ρ = density
$\Pi_y = \beta - \partial^2 U/\partial y^2 - \rho^{-1}\partial/\partial z(\epsilon\rho\partial U/\partial z)$, meridional gradient of potential vorticity of the basic state
$\beta = \partial f/\partial y$.

4. The Eady problem

The Eady problem results when (8) is restricted to $\beta = 0$, N constant, the Boussinesq approximation is made, the shear assumed linear [$U(z) = mz$], and horizontal boundaries are imposed at $z = 0, 1$:

$$\left(\tilde{z} - \frac{\tilde{\omega}}{\tilde{k}}\right)\left(\frac{\partial^2\psi}{\partial\tilde{z}^2} - \tilde{\alpha}^2\psi\right) = 0, \tag{9a}$$

$$\left(\tilde{z} - \frac{\tilde{\omega}}{\tilde{k}}\right)\psi_{\tilde{z}} - \psi = 0, \quad \tilde{z} = 0, 1, \tag{9b}$$

where the solution form $\psi(x, y, z, t) = \psi(z) \times e^{i(kx+ly-\omega t)}$ has been assumed and the following nondimensionalizations made:

$\tilde{\alpha}^2 = \alpha^2 H^2 \epsilon^{-1}$, nondimensional total wavenumber $\alpha^2 = k^2 + l^2$
$\tilde{k} = kH\epsilon^{-1/2}$
$\tilde{z} = zH^{-1}$, nondimensional height
$\tilde{t} = tm\epsilon^{1/2}$, nondimensional time
H = scale height

The tildes are dropped in what follows.

The dispersion relation follows from imposing (9b) on the solutions of (9a):

$$\frac{\omega}{k} = \frac{1}{2} \pm i\left[\alpha^{-1}\coth\alpha - \frac{1}{4} - \alpha^{-2}\right]^{1/2}.$$

The asymptotic pulse is obtained by making the Squire transformation (5) and determining the saddle point numerically from (6).

Amplification contours γ_i (Fig. 1a) reveal the pulse to be elliptical with major axis in the zonal direction and propagating with the velocity of the center of the flow.

The pulse is made up of oblique waves and, as an aid to visualization, some derived quantities are useful. These include the local real wavenumber of the oblique wave a_r (Fig. 1b). Here, a_r is defined as

$$a_r = (k_r^2 + l_r^2)^{1/2}.$$

In this case, the total wavenumber is dominated by the zonal component k_r and is symmetric about the pulse center where it obtains a minimum. The wavenumber rises toward the leading and trailing edge of the packet showing a tendency for short waves at both, in agreement with the asymptotics of Simmons and Hoskins (1979). The logarithmic singularity in k_r at the leading and trailing edge of the pulse found in that work is found in this analysis but is not resolved in Fig. 1b and is probably not of physical significance.

The phase speed of the oblique wave

$$c_a = \frac{\omega_r}{a_r}$$

increases from trailing to leading edge (Fig. 1c) with $c_a(x/t = 0.5) = 0.5$ so that the phase and group velocity of the wave at the maximum of the pulse are both equal to the velocity of the mid-level.

Figure 1d displays the angle subtended by the local oblique wave vector and the x axis: $\theta = \tan^{-1}(l_r/k_r)$. As $\omega_r > 0$ everywhere, this angle is also that of the phase velocity. West of the pulse centerline the waves propagate to the east and south, whereas east of the centerline there is a northward component.

5. The Charney problem

A more realistic model of the atmosphere, which includes both the variation of the Coriolis parameter with latitude and the effects of density stratification in the vertical while retaining the linear shear of the zonal wind, is that of Charney (1947). The conservation of pseudo potential vorticity (8a) for the geostrophic streamfunction ψ is expressed (Lindzen, *et al.*, 1980):

$$\psi_{zz} + \left\{\frac{\Pi_y}{U - \frac{\omega}{k}} - \frac{\alpha^2}{\epsilon} - \frac{1}{4H^2}\right\}\psi = 0$$

with

$$\left.\begin{aligned} \Psi &= \psi(z)e^{z/2H}e^{i(kx+ly-\omega t)} \\ \Pi_y &= \frac{\beta}{\epsilon} + \frac{U_z}{H} - U_{zz} \\ H &= \frac{RT_0}{g} \text{ the scale height} \end{aligned}\right\}.$$

The boundary conditions are (8b):

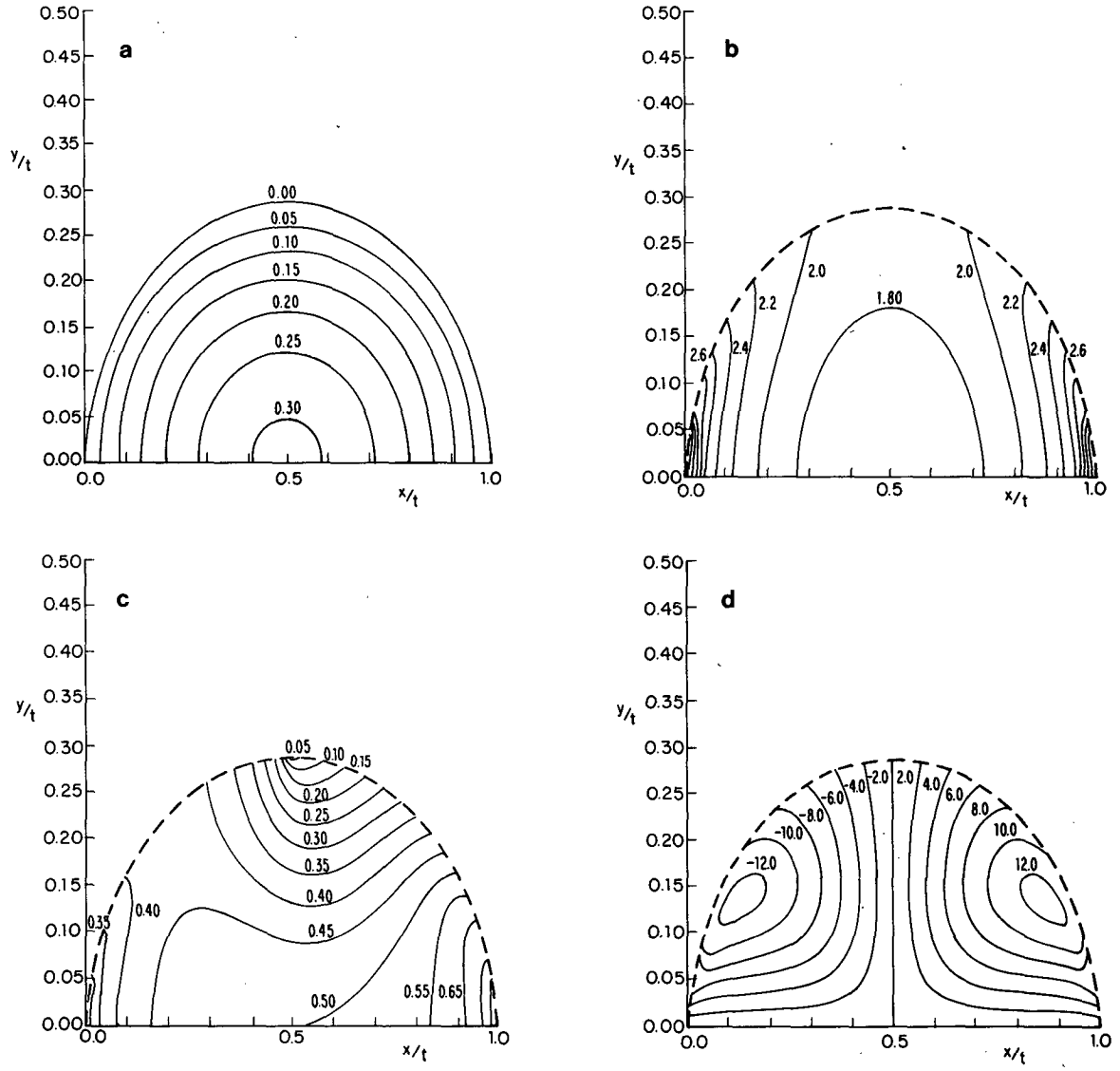

FIG. 1. (a) Local pulse growth rate γ_i for the Eady problem as a function of reference frame velocity x/t, y/t. Multiplied by any time t_0, these axes become log of pulse amplitude in the x,y plane. (b) Real part of oblique wavenumber a_r. (c) Phase speed of the oblique wave c_a. (d) Angle between the x axis and the wave vector of the oblique wave (deg).

$$\psi_z + \frac{\psi}{2H} - \frac{U_z}{U - \omega/k}\psi = 0;$$

$$z = 0; \quad \psi(z) \to 0, \quad z \to \infty.$$

We assume a linear shear $U(z) = mz$ and make the following nondimensionalizations:

$$\tilde{U} = \frac{U}{mH}, \quad \tilde{z} = \frac{z}{H}, \quad \tilde{k} = \frac{kH}{\epsilon^{1/2}}$$

to obtain

$$\psi_{\tilde{z}\tilde{z}} + \left(\frac{r+1}{\tilde{z} - \omega/\tilde{k}} - \tilde{\alpha}^2 - \frac{1}{4}\right)\psi = 0, \qquad (11a)$$

$$\psi_{\tilde{z}} + \frac{\psi}{2} + \frac{\psi}{\omega/\tilde{k}} = 0, \quad z = 0; \quad \lim_{z\to\infty} \psi(\tilde{z}) = 0, \qquad (11b)$$

where $r = \dfrac{\beta H}{\epsilon m}$.

The vertical structure equation (11a) together with the boundary conditions (11b) constitutes an eigenvalue problem which requires the dispersion relation $\Delta(\omega, \alpha) = 0$. In principle, this relation may be solved for ω complex given α, k complex by any of a number of methods including that of Lindzen *et al.* (1980). An especially convenient approximate expression was obtained by Lindzen and Rosenthal (1981), and its use in this problem is described in *F*1. A comparison

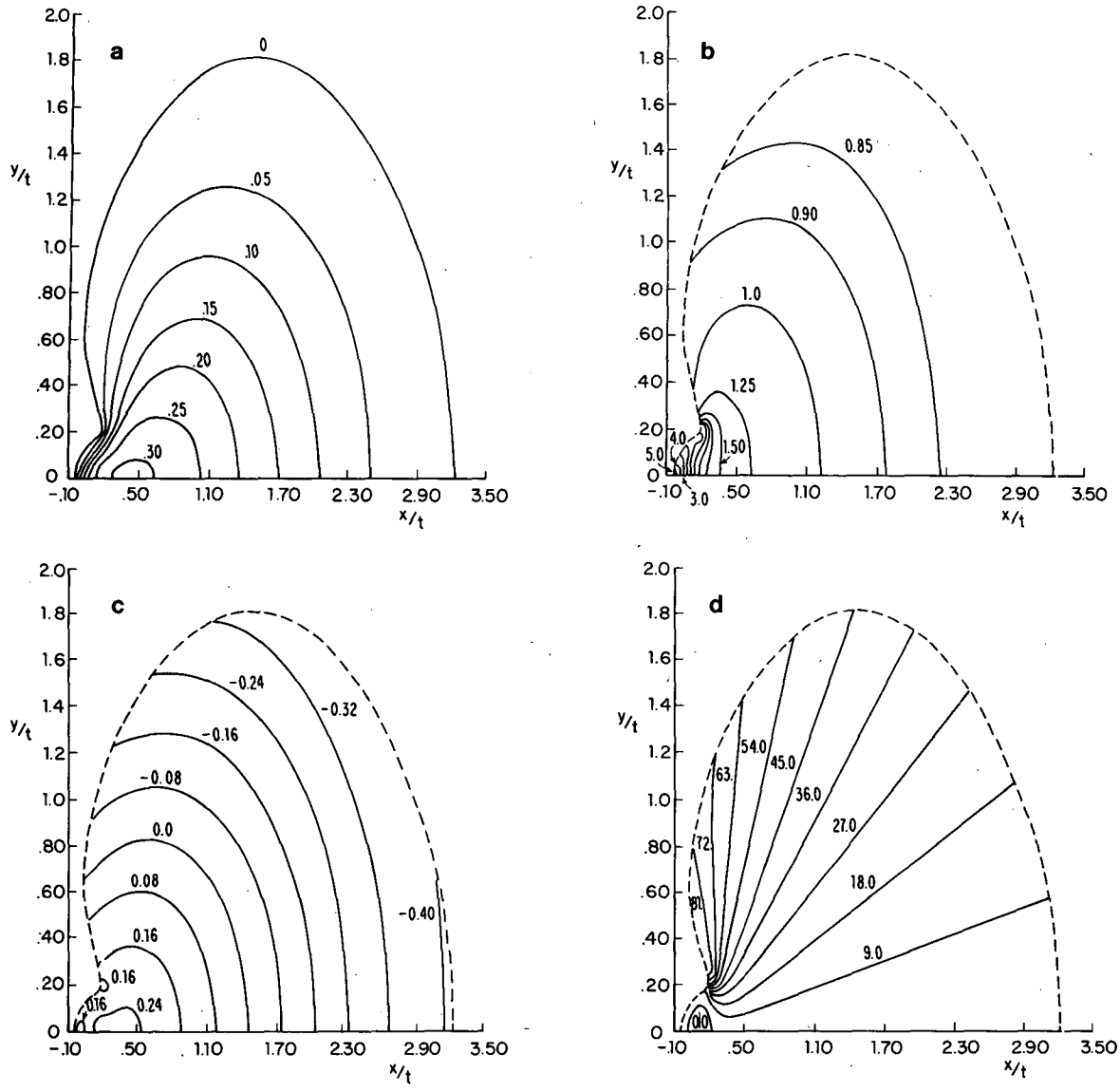

FIG. 2. As in Fig. 1, but for the Charney mode.

of the pulse derived from this approximation with that from the exact dispersion is made in Appendix A.

The Charney problem has a single stability parameter r, and a convenient choice is $r = 1.0$ for which both a high wavenumber mode (the Charney mode) and a low wavenumber mode (Burgher/Green mode) exist. These are examined separately.

6. Charney mode

In Fig. 2a γ_i for the Charney mode shows a more complicated pulse shape. The pulse maximum propagates with velocity $x/t = 0.43$ but has local phase velocity $c_x = 0.26$ so that the pulse maximum is overtaking individual high and low centers unlike in the Eady case. The shape is that of a crescent with the maximum occurring further downstream as y/t increases. There is a caustic point just outside the region of $\gamma_i = 0$ at $x/t \approx 0.1$, $y/t \approx 0.2$ which is similar to that found by Gaster and Davey (1968) in a boundary layer flow.

Total wavenumber a_r (Fig. 2b) shows a rapid decrease from trailing to leading edge along $y/t = 0$, the upstream end is characterized by short wavelengths, and the downstream by comparatively long.

The phase speed of the oblique wave c_a and the angle of the phase vector with the x axis are shown in Fig. 2c and 2d, respectively. The phase speed is seen to be less than the group speed over most of the pulse, becoming retrograde for $x/t \gtrsim 1.5$.

The Burger/Green mode gives rise to the pulse shown

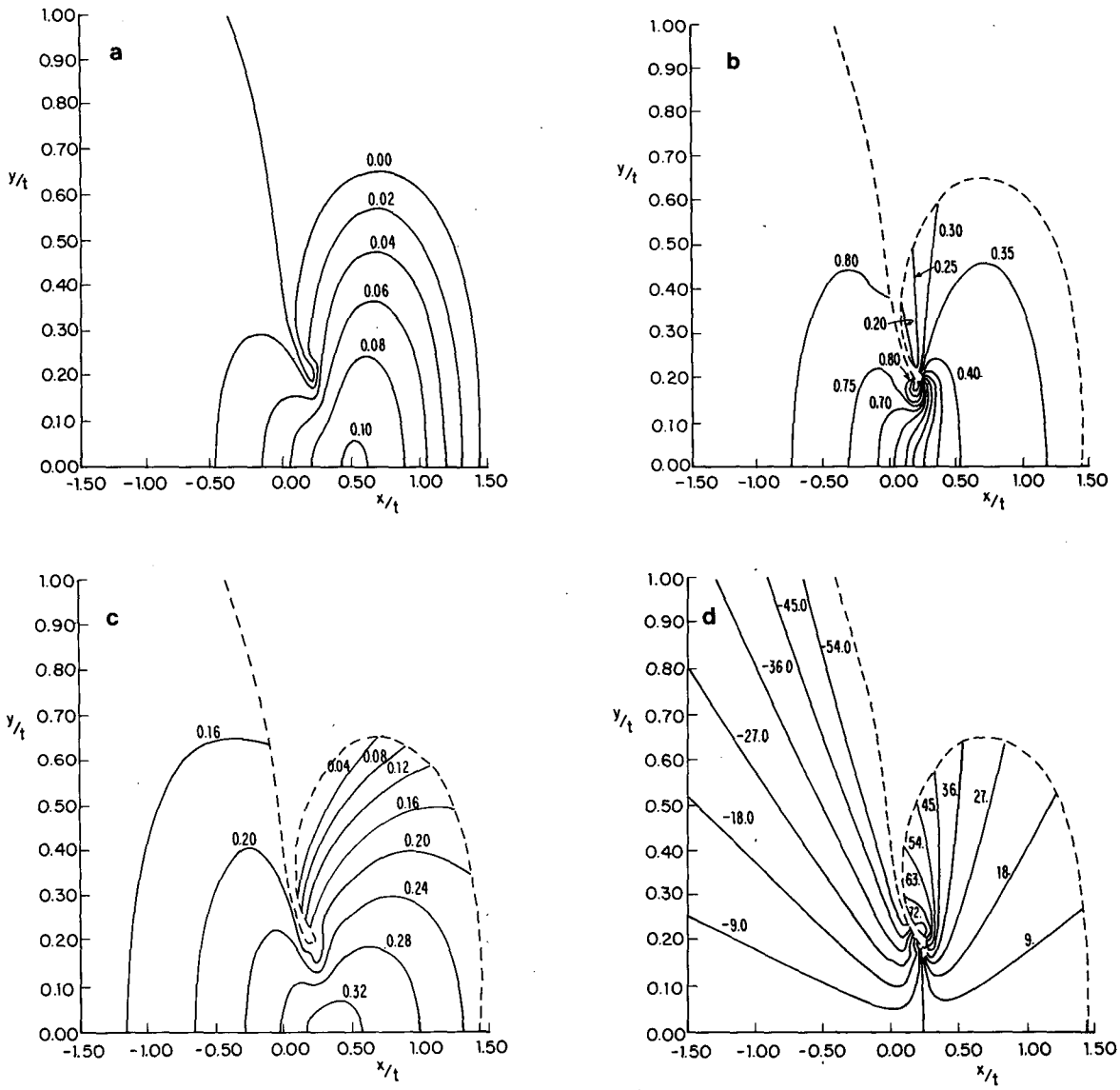

FIG. 3. As in Fig. 1, but for the Burger/Green mode.

in Fig. 3a–3d. There is pronounced upstream propagation, giving a strong absolute instability while phase speed is everywhere positive in x and shows an Eady-like southward component of propagation west of the pulse maximum and northward to the east. This mode by virtue of its strong upstream propagation can be expected to carry the upstream influence and be responsible for any absolute instability despite its relatively low growth compared with the Charney mode.

7. Vertical structure

The vertical structure of the eigenmode corresponding to the local complex wavenumber and frequency is plotted in Fig. 4 for the points $(x/t, y/t)$ listed in Table 1. In the case of the Charney mode, A is near the upstream edge of the pulse, B is the pulse maximum and C is near the downstream edge.

The upstream edge is characterized by short waves with shallow vertical penetration while the downstream edge exhibits a remarkable maximum in the upper troposphere and little phase tilt. Similar results were obtained by Simmons and Hoskins (1979) from integrations of the equations of motion with a localized initial perturbation and are found in observed vertical structures (Lau, 1978).

Burger/Green mode structures show less variation, being similar to that of the maximum point which is labeled A in Fig. 5. The leading edge wave (B in Fig. 5) is remarkable for its negative phase tilt over much of the upper troposphere portion of the wave. These eastward tilts may be expected to give rise to

TABLE 1. Eigenmode parameters plotted for Charney and Burger/Green modes.

	Label	x/t	y/t	k_r	k_i	ω_r	ω_i
Charney (Fig. 4)	A	0.02	0.0	6.91	−2.60	0.857	0.060
	B	0.45	0.0	1.41	0.0	0.371	0.322
	C	3.00	0.0	0.777	0.045	−0.368	0.137
Burger/ Green (Fig. 5)	A	0.50	0.0	0.405	0.00	0.13	0.097
	B	1.40	0.0	0.34	0.18	0.08	0.256
Charney $l = 2.0$ (Fig. 6)	A	0.02	0.0	7.67	−1.89	0.854	0.058
	B	0.15	0.0	2.34	0.00	0.544	0.169
	C	0.42	0.0	0.97	1.00	0.209	0.441

negative heat fluxes in the upper troposphere (Appendix B) such as are observed downstream of major storm tracks (Lau, 1978).

It is interesting to compare these vertical structures with what is found for the asymptotic pulse of the Charney problem restricted to the gravest meridional mode in a channel of width $L = \pi$ (F1, Fig. 9). The points of interest are listed in Table 1 and include: A near the upstream edge, B the pulse maximum, and C near the leading edge. The vertical structure (Fig. 6) shows the tendency for the vertical scale to grow with the wavelength along the pulse and exhibits the phase reversal in the upper troposphere which characterizes waves near the downstream edge of the pulse.

8. Interval of validity

The use of linear asymptotics must raise the question of determining the interval in time during which the solutions are valid. This interval is bounded below by the time required for the most favored modes to rise out of the initial spectrum to dominate the solution. It is bounded above by the time beyond which nonlinear effects on the pulse propagation cannot be ignored. An estimate of these bounds may be made by noting that if no mode is initially strongly favored the lower is of the order of an advection period for the wavelength in question (Farrell, 1982b). For a given shear this will vary along the pulse with the short wavelengths being set up quickly at the upstream end and the longer downstream waves requiring proportionately more time. The upper bound depends on the amplitude of the initial disturbance and, as is usual with problems involving nonlinearity, is best determined by performing a numerical integration. The results of Simmons and Hoskins (1979), their Fig. 1 and Fig. 3, show the linear pulse solutions capture the essential features of the wavetrain development even at times for which the central maximum is fully nonlinear.

9. Summary and discussion

The asymptotic three-dimensional structure of baroclinic pulses on an f-plane and β-plane have been obtained. Although inhomogeneities in the atmosphere could be expected to prevent the establishment of such a pulse in pure form, these results suggest some interpretations:

1) The meridional extent of an asymptotic pulse on an infinite β-plane is typically comparable to its zonal extent so that the tendency for baroclinic waves to be restricted in the north/south direction must result from the structure of the basic state flow or from sphericity effects.

2) At any point in a wave train there corresponds a local value for the complex parameters ω, k, l. In turn, the vertical structure of the wave and fluxes induced by it are determined by these local parameters. There is a tendency to compare vertical structures of observed waves to temporal normal modes, but as we have seen, this is not justified except at the single point of the pulse maximum. For instance, upper troposphere maximum amplitudes and negative heat fluxes are predicted for downstream waves in contrast to temporal normal mode results for the Charney problem for which stream function maximums are all at the ground and heat fluxes northward.

3) The storm track progression from short, shallow "intermediate scale" lows to mature cyclones to barotropic structures with upper level maximums and southward heat fluxes in mid-troposphere (Lau, 1978) is reproduced by the pulse asymptotics without recourse to nonlinear modification of the mean flow.

4) There is, for some (k, ω) corresponding to a ray $(x/t, 0)$ the coincidence of phase velocity and group velocity. This coincidence does not occur for neutral barotropic Rossby waves for which

$$c_g = c_x + \frac{2\beta k^2}{(k^2 + l^2)^2} > c_x.$$

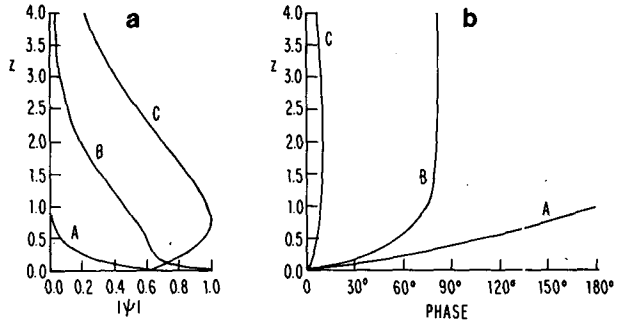

FIG. 4. The vertical structure (a) amplitude, and (b) phase of the Charney mode pulse near the upstream edge A, at the pulse maximum B, and near the leading edge C.

Such a wave could be the preferred mode for a region of forcing that is geographically localized as it could satisfy the resonance condition $U(0) + c_x = 0$, and yet its energy remains in the forcing region. The Eady problem can be seen to require $U(0) = -0.50$ while the Charney gives $U(0) = -0.28$ and the Burger/Green $U(0) = -0.33$. These easterly surface flows are probably too great to occur in the atmosphere so that such resonance is likely confined to barotropically unstable flows (Lindzen *et al.*, 1983).

5) The analysis of synoptic scale disturbances focuses on the phase velocity of the waves as marked by the movement of the low centers. The attendant packet group velocity may be of either sign relative to the phase velocity so that the "seed" disturbance for a cyclogenesis may come from a downstream or upstream cyclone group and not *in situ* noise.

6) Downstream of a cyclogenesis region, the disturbance would tend to be made up of the leading edge waves which are nearly barotropic and possess rapid eastward group velocity together with small or even retrograde phase velocity.

There is a further discussion of points 5 and 6 in relation to model integrations in Simmons and Hoskins (1979) and observations of Hovmöller (1949) and Krishnamurti *et al.*, (1977) are illustrative.

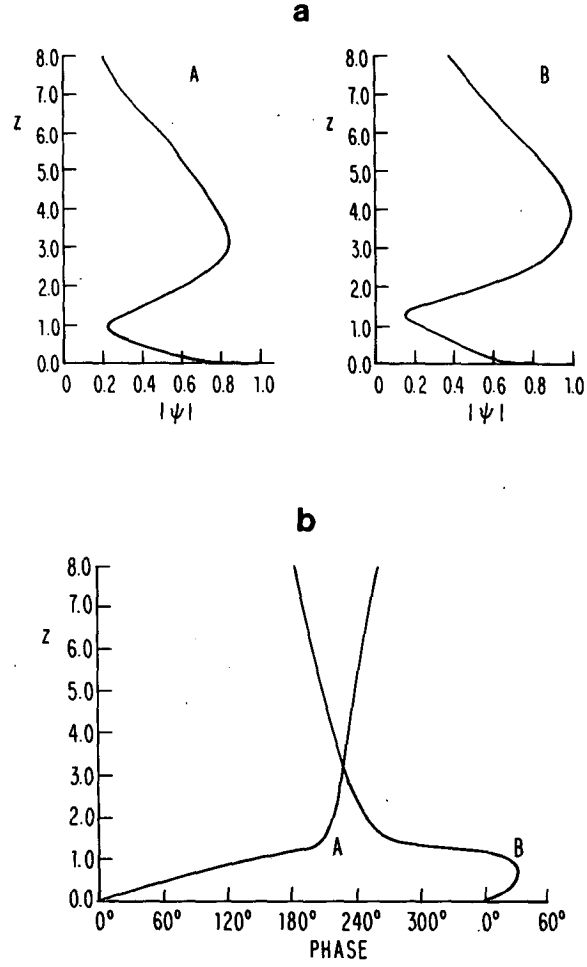

FIG. 5. As in Fig. 4, but of the Burger/Green mode pulse at pulse maximum A, and at the leading edge B.

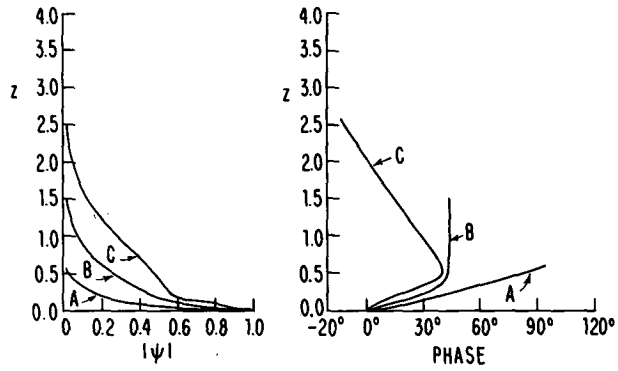

FIG. 6. The vertical structure of the Charney mode restricted to $l = 2.0$, near the upstream edge A, at pulse maximum B, and near the leading edge C.

Acknowledgments. The author wishes to thank Dr. R. S. Lindzen and Dr. L. O. Merkine for helpful criticism. This work was supported by NASA Grant NGL-22-007-228.

APPENDIX A

Comparison of the Exact and Approximate Pulse

The exact dispersion relation for the Charney problem obtained by the method of Kuo (1979) may be used to obtain a pulse solution. The pulse for this exact solution (Fig. A1) is nearly identical with the

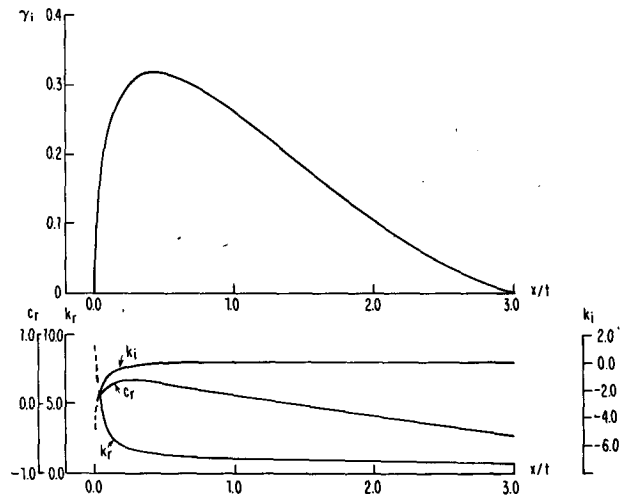

FIG. A1. (a) local pulse growth rate γ_i for $l = 0$, $r = 1.0$ as a function of velocity x/t. (b) complex wavenumber k, together with phase speed c_r, across the pulse.

approximate pulse (Farrell, 1982, Fig. 5) but for the elimination of the slight upstream propagation in the Charney mode.

APPENDIX B

Heat Flux for Complex Zonal Wavenumber

The heat flux for complex zonal wavenumber is

$$v'\theta' = \mathrm{Re}(\Psi_x)\,\mathrm{Re}(\Psi_z) = \mathrm{Re}(ik\Psi)\,\mathrm{Re}(\Psi_z). \quad \text{(B1)}$$

With the substitution of

$$\Psi = \psi(z)e^{z/2}e^{i(kx-\omega t)} = |\psi(z)|e^{i\alpha(z)+z/2}e^{i(kx-\omega t)},$$

(B1) may be reduced to

$$v'\theta' = \overbrace{|\psi(z)|^2 e^{z-2k_i x+2\omega_i t}}^{A}\left[\frac{k_r\alpha_z - k_i G}{2} + \frac{|k|(\alpha_z^2+G^2)^{1/2}}{2}\cos(2\delta+\gamma)\right], \quad \text{(B2)}$$

where

$$\left.\begin{aligned}\delta &= k_r x + \alpha - \omega_r t\\ G &= \frac{d}{dz}\ln(e^{z/2}|\psi(z)|)\\ \gamma &= \tan^{-1}\left(\frac{k_r G - k_i\alpha_z}{k_i G + k_r\alpha_z}\right)\end{aligned}\right\}.$$

Taking the Charney $l = 2$ downstream edge example (Fig. 6, curve C) and evaluating at $z = 1.0$:

$$k_r = 0.97, \quad k_i = 1.00, \quad \alpha_z = -0.52, \quad G = -0.1.$$

The sign of the flux is determined by the quantity in brackets in (B2):

$$v'\theta' = A[-0.20 + 0.52\cos(\gamma + 2\delta)].$$

The flux of heat is biased negatively (toward the south) at this level although the exponential decay in x makes this result phase dependent.

REFERENCES

Briggs, R. J., 1964: *Electron-stream Interaction with Plasmas*, Chapter 2. MIT Press, 8–46.

Charney, J. G., 1947: The dynamics of long waves in a baroclinic westerly current. *J. Meteor.*, **4**, 135–162.

Eady, E. T., 1949: Long waves and cyclone waves. *Tellus*, **1**, 33–52.

Farrell, B. F., 1982a: Pulse asymptotics of the Charney baroclinic instability problem. *J. Atmos. Sci.*, **39**, 507–517.

——, 1982b: The initial growth of disturbances in a baroclinic flow. *J. Atmos. Sci.*, **39**, 1663–1686.

Gaster, M., 1965: On the generation of spatially growing waves in a boundary layer. *J. Fluid Mech.*, **22**, 433–441.

——, and A. Davey, 1968: The development of three-dimensional wave-packets in unbounded parallel flows. *J. Fluid Mech.*, **32**, 801–808.

Hogg, N. G., 1976: On spatially growing baroclinic waves in the ocean. *J. Fluid Mech.*, **78**, 217–235.

Hovmöller, E., 1949: The trough-and-ridge diagram. *Tellus*, **1**, 62–66.

Kuo, H. L., 1979: Baroclinic instabilities of linear and jet profiles in the atmosphere. *J. Atmos. Sci.*, **36**, 2360–2378.

Krishnamurti, T. N., J. Molinari, H.-L. Pan and V. Wong, 1977: Downstream amplification and formation of monsoon disturbances. *Mon. Wea. Rev.*, **105**, 1281–1297.

Lau, N. C., 1978: On the three-dimensional structure of the observed transient eddy statistics of the northern hemisphere wintertime circulation. *J. Atmos. Sci.*, **35**, 1900–1923.

Lindzen, R. S., and A. J. Rosenthal, 1981: A WKB asymptotic analysis of baroclinic instability. *J. Atmos. Sci.*, **38**, 619–629.

——, B. Farrell and K.-K. Tung, 1980: The concept of wave overreflection and its application to baroclinic instability. *J. Atmos. Sci.*, **37**, 44–63.

——, B. Farrell and A. J. Rosenthal, 1983: Absolute barotropic instability and monsoon depressions. *J. Atmos. Sci.*, **40**, 1178–1184.

McIntyre, M. E., 1970: On the non-separable baroclinic parallel flow instability problem. *J. Fluid Mech.*, **40**, 273–306.

Merkine, L. O., 1977: Convective and absolute instability of baroclinic eddies. *Geophys. Astrophys. Fluid Dyn.*, **9**, 129–157.

——, and Shafranek, 1980: The spatial and temporal evolution of localized unstable baroclinic disturbances. *Geophys. Astrophys. Fluid Dyn.*, **16**, 175–206.

Pedlosky, J., 1979: *Geophysical Fluid Dynamics*, Springer-Verlag, 624 pp.

Simmons, A. J., and B. J. Hoskins, 1979: The downstream and upstream development of unstable baroclinic waves. *J. Atmos. Sci.*, **36**, 1239–1254.

Stone, P. H., 1969: The meridional scale of baroclinic waves. *J. Atmos. Sci.*, **26**, 376–389.

Squire, H. B., 1933: On the stability of three-dimensional disturbances of viscous flow between parallel walls. *Proc. Roy. Soc. London*, **A142**, 621–628.

Thacker, W. C., 1976: Spatial growth of Gulf Stream meanders. *Geophys. Fluid Dyn.*, **7**, 271–295.